Solar Energy 265 (2023) 112125

Contents lists available at ScienceDirect

Solar Energy

journal homepage: www.elsevier.com/locate/solener

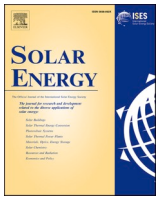

Comprehensive analysis of dust impact on photovoltaic module temperature: Experimental insights and mathematical modeling

Hussam Almukhtar [a,*], Tek Tjing Lie [a], Wisam A.M. Al-Shohani [b]

[a] Department of Electrical and Electronic Engineering, Auckland University of Technology, Auckland 1010, New Zealand
[b] Department of Mechanical Power Engineering, Engineering Technical College, Middle Technical University, Baghdad 53172, Iraq

A B S T R A C T

Dust accumulation substantially impacts the efficiency and thermal behavior of photovoltaic (PV) modules. Addressing a current knowledge gap, this article presents a comprehensive assessment of the impact of dust on PV module temperature. This endeavor includes a combination of systematic experiments with a novel developed mathematical model that uniquely incorporates key dust parameters such as emissivity, absorbance, and transmittance. The model enhances accuracy in estimating PV module temperature compared to existing mathematical models, which often overlook heat absorption due to dust and specific dust characteristics. These parameters are measured using specialized devices to ensure realistic values. Outdoor experiments are conducted to validate the model's predictions under real weather conditions, further highlighting the importance of accurate PV temperature estimation in dusty environments. Additionally, a comparative analysis is performed with existing mathematical models for PV temperature prediction, demonstrating the superior performance of the proposed model, which achieves the lowest average prediction error (mean absolute error of 1.4). These findings provide valuable insights into the estimation of PV temperature in dusty conditions, bridging the gap between theoretical modeling and practical application and underscoring the novelty and innovation introduced in this research.

1. Introduction

Climate change and increasing energy demand have heightened the global importance of seeking sustainable energy solutions [1]. Among the array of renewable energy alternatives, PV technology has emerged as a transformative force capable of converting solar energy into electricity [2]. With the advent of cleaner energy and reduced environmental impact, this technology has fostered the possibility of a more sustainable future [3,4]. However, PV technology's performance and efficiency are closely linked to weather patterns, material properties, and environmental factors [5].

For instance, one of the most significant threats to PV technology's performance is the deposition of dust on PV module systems [6]. Dust affects energy absorption, heat dissipation, and thermal equilibrium on module surfaces, thereby influencing the operational dynamics of PV systems [7,8]). Dust accumulation is more frequent in arid and semi-arid regions like the Middle East and North Africa, which boast high solar energy potential [9]. The accumulation of dust particles on PV module surfaces diminishes the intensity of incident sunlight reaching the solar cells, resulting in reduced power output [10]. This phenomenon has been extensively studied, with numerous research papers reporting significant declines in PV system performance due to dust accumulation with a reduction of up to 50 % depending on dust levels [7,11]. Furthermore, dust presents a notable challenge to the efficiency of solar technologies like CSP systems. The accumulation of dust on the CSP systems can scatter and absorb sunlight, reducing the amount of solar radiation reaching the target. This can lead to decreased thermal efficiency and reduced electricity generation [12,13].

Furthermore, dust accumulation can create uneven temperatures and hot spots, leading to overall higher temperatures in PV modules and decreased efficiency [7]. Understanding the effects of dust accumulation and its interaction with temperature changes is vital for enhancing PV system efficiency and reliability [14]. Consequently, accurate temperature predictions are pivotal for comprehending and enhancing solar energy system performance [15]. Dust buildup is an essential key factor affecting PV module efficiency [16]. The extent of this impact varies based on the specific geographic location and local environmental conditions [17]. This following section offers a concise overview of the current state of research in estimating PV temperature, emphasizing the evolution of approaches and identifying the existing challenges.

Accurate temperature prediction for PV modules is crucial for enhancing the performance and efficiency of PV systems. Numerous studies have developed methods and models for estimating PV temperature, taking various environmental factors into consideration. This section provides an overview of the existing literature, emphasizing key approaches and challenges.

* Corresponding author.
E-mail addresses: hussam.almukhtar@autuni.ac.nz (H. Almukhtar), tek.lie@aut.ac.nz (T.T. Lie), wam@mtu.edu.iq (W.A.M. Al-Shohani).

https://doi.org/10.1016/j.solener.2023.112125
Received 12 September 2023; Received in revised form 10 October 2023; Accepted 15 October 2023

Early research studies in PV temperature estimation primarily focused on establishing simple empirical relationships between PV module temperature, solar irradiation, and ambient temperature [18]. While these empirical correlations laid the foundation for understanding PV module temperature behaviour, they often lacked precision. As research advanced, more sophisticated models were developed, incorporating additional variables that influence PV temperature. These models tackled the complexities by considering various environmental factors including ambient air temperature, solar irradiation, and wind speed [19].

Furthermore, studies have highlighted the impact of optical properties and dust accumulation on PV temperature. Some researchers have emphasised the necessity of accounting for the reduction of light caused by dust in temperature prediction models, given its significant effect on light scattering. This led to the inclusion of dust-related factors in temperature estimation equations, such as transmittance [20]. Additionally, efforts to enhance PV temperature predictions included analytical models that incorporated weather conditions and principles of heat transfer, such as natural convection and radiation, as demonstrated by Tomar et al. [21]. This approach bridged the gap between theoretical analysis and experimental validation, providing deeper insights into PV temperature behaviour [21].

Mathematical models have expanded to encompass electrical, thermal, and optical elements, offering a comprehensive perspective by accounting for the intricate relationships among various parameters. Gupta et al. [10] developed a comprehensive model that predicts PV temperature by integrating electrical, thermal, and optical elements, recognising the complex nature of temperature behaviour in PV modules.

In summary, research has evolved from early studies focused on ambient factors to advanced approaches that consider heat transmission processes, optical properties, and the effects of dust accumulation. These advancements reflect ongoing efforts to improve PV temperature estimation, thereby enhancing the accuracy and reliability of predicting PV module behaviour under diverse climatic conditions. Table 1 provides equations and correlations derived from published research, facilitating the calculation of PV temperatures while accounting for various environmental variables, optical module properties, and heat transport equations.

T_{PV} represents the temperature of the PV module. Ta is the ambient temperature surrounding the PV module. G denotes the solar irradiance received by the module. ν is the wind speed impacting the module. ω symbolizes humidity. A is the absorptivity coefficient of the module. η symbolizes the efficiency of the PV module. τ represent the transmisstance. Ul is the overall heat loss coefficient of the module. Uv denotes a coefficient related to wind speed. γ and β are a coefficient indicating thermal impact on the electrical PV coefficient. σ representing the Stefan-Boltzmann constant. Finally, hc and hr are the convective and radiative heat transfer coefficients, respectively.

Achieving optimal performance in solar energy systems necessitates

Table 1
Equations and correlations for estimating photovoltaic temperature from published research.

Ref.	Parameters	Equation	Eq. No
[18]	T_a	$T_{PV} = 0.0282G + Ta$	(1)
[22]	T_a, G	$T_{PV} = 30 + 0.0175(G-300) + 1.14(Ta-25)$	(2)
[23]	T_a,G	$T_{PV} = Ta + (3 \times G/1000)$	(3)
[24]	c	$T_{PV} = Ta + 0.022G(1+0.009Ta)(1-0.063\nu)$	(4)
[19]	T_a,G,ν	$T_{PV} = 3.81 + 0.0282G + 1.31Ta - 1.65\nu$	(5)
[25]	T_a,G,ν	$T_{PV} = 0.943 \times Ta + 0.0195 \times G - 1.528 \times \nu + 0.3529$	(6)
[26]	T_a,G,ν	$T_{PV} = 3.12 + 0.025G + 0.899Ta - 1.3\nu$	(7)
[27]	T_a,G,ν	$T_{PV} = 4.3 + 0.0028G + 0.943Ta - 1.528\nu$	(8)
[28]	T_a,G,ν	$T_{PV} = 0.943 \times Ta + 0.028 \times G - 1.528 \times \nu + 4.3$	(9)
[29]	T_a,G,ν	$T_{PV} = 1.4 \times Tatm + 0.1(G-500) - \nu^{0.8}$	(10)
[30]	T_a,G,ν	$T_{PV} = Ta + (G/(27.307 + 3.0381\nu))$	(11)
[23]	T_a,G,ν	$T_{PV} = G.\{e^{-3.47-.075\nu}\} + T_a + 3 \times G/1000$	(12)
[31]	T_a,G,ν	$T_{PV} = 2.08 + 0.0182G + 1.038Ta - 1.13\nu$	(13)
[32]	T_a,G,ν,ω	$T_{PV} = Ta + G \times 0.32 \times \frac{w}{8.91} + 2 \times v$	(14)
[14]	T_a,G,ν,ω	$T_{PV} = 30.60 + 0.409Ta = + 0.014G - 0.15w - 0.377\nu$	(15)
[33]	T_a,G,ν,ω	$T_{PV} = Ta + Bh\left[\frac{G}{800}(NOCT-20)\right] + Ch(w_h - w_1)$	(16)
[34]	T_a,G,ν,ω	$T_{PV} = \frac{1}{3} \times [3.941Ta + 281.7 \times (G/1000)^{0}.01088 + 269.1w^{0}.005602 - 0.1761v + 275.9] - 273.15$	(17)
[20]	T_a, G,,α,η	$T_{PV} = Ta + G\alpha[1-\eta]/29$	(18)
[35]	T_a,G,ν,τ,α,η	$T_{PV} = Ta + ((\alpha.G\ (1-\eta))/((12.85 + 1.06v) \times 2))$	(19)
[21]	T_a, G,ν, τ,α,η, U_l	$T_{PV} = Ta + G\frac{\tau.\alpha}{U_L}[1-\eta]U_l = hr + hc,\ h_c = 2.8 + 3 \times V,$ $h_r = \epsilon_{PV}\sigma\left(T_{PV}+T_{sky}\right)\left(T_{PV}^2 + T_{sky}^2\right)$	(20)
[36]	T_a, G,ν, τ,α,η, U_l	$T_{PV} = \frac{U_{PV}T_a + G \times (\alpha_c.\tau - \eta_o - \beta\eta_{ref}T_{ref})}{U_{PV} - G\beta\eta_{ref}}$UPV = 26.6 + 2.3v	(21)
[15]	T_a,G,ν, τ,α,η, U_l	$T_{PV} = \frac{U_V T_a + G \times (\alpha_c\tau - \eta_{stc}(1-\beta T_{ref})(1+\gamma Ln(\frac{G}{Go}))}{U_v + \beta\eta_{ref}((1+\gamma Ln(\frac{G}{Go})G}$Uv = 26.6 + 2.3 v, $(\tau\alpha) = 0.81$	(22)
King et al. cited in [15]	T_a,G,ν, τ,α,η, U_l	$[(\tau\alpha) - \eta]G = U_V(T_{PV} - T_a)$Uv = 26.6 + 2.3 v,	(23)

a comprehensive understanding of the diverse methods and equations employed in the calculation of PV module temperatures. While previous research has explored the effects of dust on transmittance, it frequently neglects other crucial dust-related factors, including absorption and emittance. These parameters are of utmost importance as they directly impact the thermal behaviour of PV. This research is geared towards enhancing the precision of PV temperature estimations, consequently bolstering the effectiveness of PV technology, by addressing these often-overlooked factors. Comprehending the intricate effects of dust accumulation is essential to estimate PV module temperature.

Therefore, this study employs detailed experiments and advanced mathematical models to investigate the impact of dust on PV module temperature.

- Detailed investigations have been made into the influence of dust characteristics on light absorption, transmission, and heat dissipation. Using UV–vis Spectroscopy, transmittance and absorbance of the dust layer are measured. Concurrently, the emissivity of dust-coated PV surfaces is determined using the advanced INGLS TIR100-2 measuring device.
- Building on these empirical findings, the study introduces a novel mathematical model that integrates dust characteristics, meteorological variables, and PV parameters. This comprehensive framework provides precise temperature estimations, addressing gaps in existing studies which often overlook the role of dust characteristics on internal heat transfer processes within PV modules.
- The approach extends from theoretical foundations to practical applications, validating the developed model by comparing its predictions against actual temperature variations observed in dusty PV systems.
- In a comparative evaluation, the model demonstrates superior performance over existing mathematical models, especially in dust weather condition, highlighting its potential for broader applicability and enhanced accuracy.

2. Methodology

This paper introduces an approach to establish a mathematical correlation between dust properties and the thermal performance of PV modules. The methodology comprises two interrelated components: a theoretical framework involving mathematical correlations and an empirical approach that validates these correlations. The study is conducted in an arid environment, encompassing the location, experimental setup, and procedure for dust collection during regional storms. Analytical techniques are employed to characterize the chemical composition of the collected dust, along with measurements of its emissivity and optical properties. Outdoor experiments involving various PV modules are conducted to validate the developed mathematical correlations. Subsequent sections will offer a comprehensive overview of these key facets of the methodology.

2.1 Development of mathematical correlations

This study endeavours to construct a robust mathematical model that comprehensively addresses the intricate correlation between dust accumulation and PV module temperature. The research employs two interconnected strategies to explore the relationship between dust accumulation and PV module temperature. The first strategy prioritises by treating the PV module as a single-layer structure. Conversely, the second strategy involves a more comprehensive analysis that considers the PV module's five-layer composition. This advanced approach incorporates heat transfer mechanisms within each layer to ensure the model accurately mirrors real-world conditions. The model is meticulously tuned to encompass both the complex thermal behaviours of the PV module and the distinctive characteristics of its multiple layers.

2.1.1. Simplified dusty PV module energy balance equation

Initially, the study concentrates on treating the PV module as a single layer to simplify the comprehension of the energy balance equation and to provide a more straightforward representation. This approach facilitates a more concise demonstration of the energy balance equation for a dusty PV glass surface. Fig. 1 illustrates that solar energy is converted into electrical power, with significant portion remaining as heat. Typically, this heat is released into the atmosphere through convection and radiation from both sides of the PV module.

The energy balance equations are formulated under specific assumptions governing heat transfer. These assumptions encompass one-dimensional heat transfer within a single PV layer and steady-state conditions. These simplifications are made to streamline mathematical calculations while retaining the core understanding of the PV module's thermal behaviour. As evident in Fig. 1, the energy balance equation for the dusty PV surface can be represented by Eq. (24) as follows:

$$\begin{aligned} Q_{in} &= Q_{out} \\ Q_{abs}(dust + PVcell) &= \mathrm{Q}_{gen} + (Q_{conv} + Q_{rad}) \\ \alpha_d G + \tau\alpha_c G(1-\eta_{PV}) &= 2h(T_{PV} - T_a) + 2h_r(T_{PV} - T_{sky}) \\ T_{PV} &= \frac{[\alpha_d G + \tau\alpha_c G(1-\eta_{PV}) + 2h_r Tsky + 2h_c T_a]}{2(h+hr)} \end{aligned} \tag{24}$$

where, $\mathrm{Q_{in}}$ represents the energy input to the PV module, which includes the heat absorbed by the dusty layer and PV cell ($\mathrm{Q_{abs}} = \alpha_d G + \tau\alpha_c G$). $\mathrm{Q_{out}}$ represents the energy output from the PV layer, including heat loss to the atmosphere through convection ($\mathrm{Q_{conv}} = \mathrm{Q_{convection}}$) and radiation ($\mathrm{Q_{rad}} = \mathrm{Q_{radiaition}}$). G represents solar radiation, h and h_r (convection and radiation heat transfer coefficients) can be calculated as described in Eqs. (25) and (26) [37]. Additionally, the properties of the PV module include absorption coefficient (α_c), emissivity (ϵ_{PV}), and temperature of PV module (T_{PV}). T_a represents ambient temperature, and T_{sky} represents sky temperature, which can be calculated by Eq. (27) as follows [38]:

$$h_r = \epsilon_{PV}\sigma(T_{PV}^2 + T_{sky}^2)(T_{PV} + T_{sky}) \tag{25}$$

$$h = 11.9 + 2.2\nu \tag{26}$$

$$\mathrm{T_{sky}} = 0.0552\mathrm{Ta}^{1.5} \tag{27}$$

This simplified energy balance equation captures the fundamental heat transfer processes between the dusty PV glass surface and its surroundings. The equation takes into consideration the absorbed solar radiation, heat conduction, convection, and radiation, offering a concise representation of the thermal interactions responsible for the temperature increase of the PV module due to dust accumulation. Further elaboration on the intricate thermal behaviour of dust will be comprehensively discussed in the subsequent section, providing a detailed insight into its effects on the PV temperature.

The temperature equation for the clean PV module remains identical to that of the dusty scenario, except it omits the initial temperature affected by dust absorption, denoted as $\alpha_d G$.

2.1.2. Five-Layer structure PV module energy balance equation

This subsection focuses on the thermal model, which takes into account the distinct layers, including the PV module. These layers comprise the glass, EVA1, PV cell, EVA2, and Tedlar, as depicted in Fig. 2A. Each layer is treated as a separate node in the model, and energy balance equations are established for each node, as shown in Fig. 2B. These equations encompass each layer's energy input and output and incorporate various environmental factors to replicate real weather conditions.

The energy balance equations are formulated under specific assumptions concerning the heat transfer process. These assumptions encompass one-dimensional heat transfer within each layer, steady-state conditions with constant temperature within each layer, and negligible

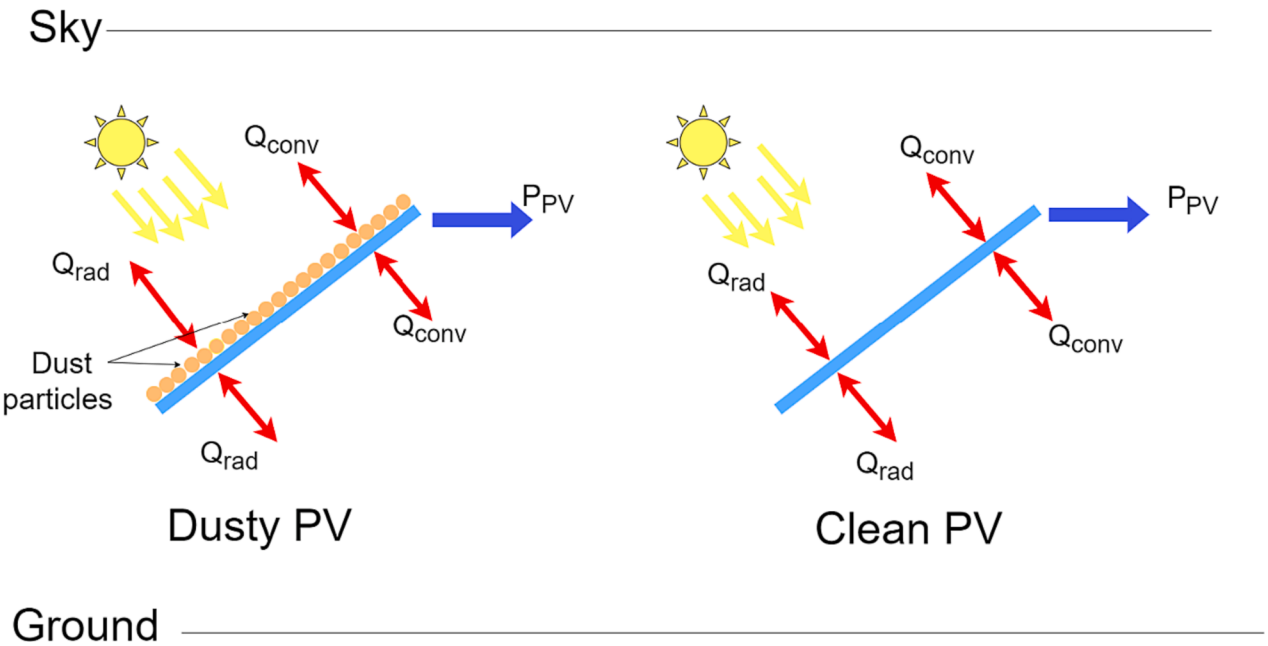

Fig. 1. Comparative visualization of energy flow input and output analysis in clean and dust PV modules.

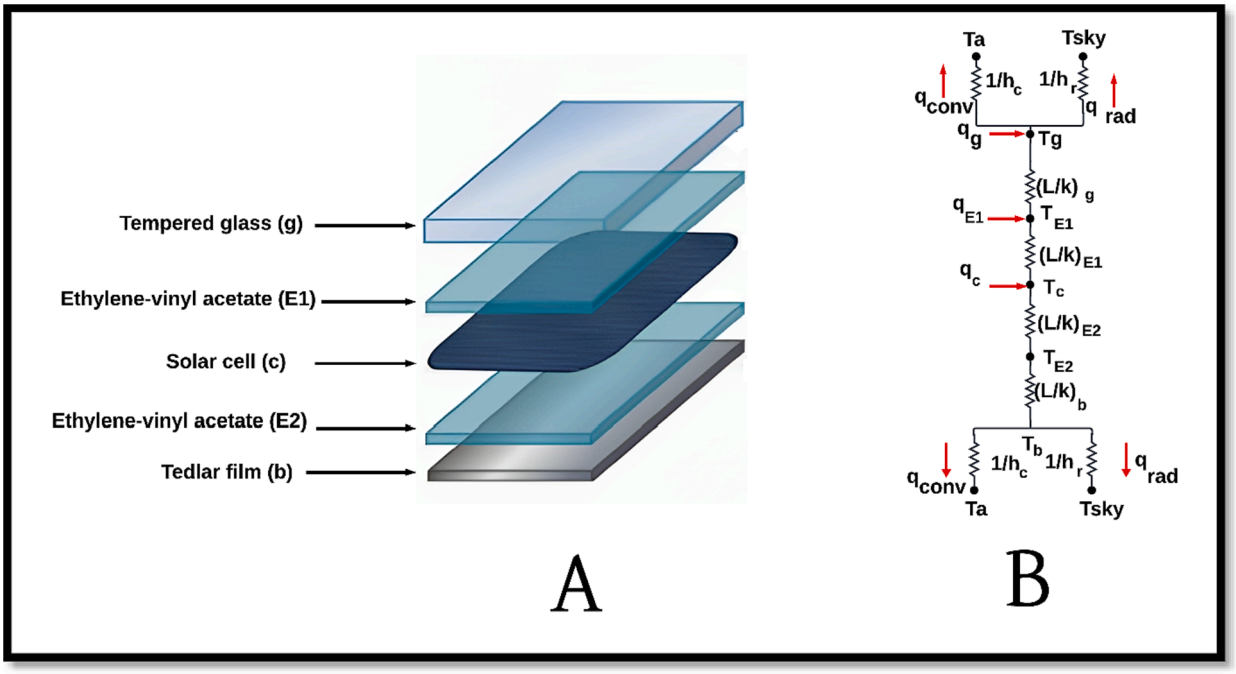

Fig. 2. A. Typical solar module components materials and B. Thermal equivalent circuit.

temperature variations across the layers. These simplifications are introduced to streamline the mathematical calculations while still capturing the fundamental thermal behaviour of the PV module.

The analysis comprises two stages: Firstly, the thermal model is applied to analyse the clean PV module, representing dust-free conditions. This initial analysis unveils the PV module's temperature distribution and performance characteristics under ideal conditions. Secondly, the model is expanded to account for dust accumulation on the PV surfaces. By incorporating the effects of dust particles, the thermal model quantifies the resulting temperature and performance changes. The derived energy balance equations facilitate a comparison with the baseline, shedding light on the impact of dust accumulation on the module's behaviour.

2.1.2.1. Clean PV. The energy balance equation for the PV glass surface can be represented by Eq. (28) as follows:

$$\begin{gathered} Q_{in} = Q_{out} \\ Q_{abs} + Q_{cond} = (Q_{conv} + Q_{rad}) \\ \alpha g G + \frac{k_g}{L_g}(T_{E1} - T_g) = \mathrm{h}\left(T_g - T_a\right) + \epsilon_g \sigma\left(T_g^4 - T_{sky}^4\right) \end{gathered} \tag{28}$$

Q_{in} represents the energy input to the glass layer, which includes the heat absorbed by the glass ($Q_{abs} = \alpha_g G$) and the heat conducted from the

second layer EVA ($Q_{con} = Q_{conduction}$). Q_{out} represents the energy output from the glass layer, including heat loss to the atmosphere through convection ($Q_{conv} = Q_{convection}$) and radiation ($Q_{rad} = Q_{radiation}$). T_{E1} represents the temperature of the EVA1 layer. Additionally, the properties of the glass layer include absorption coefficient (αg), thickness (L_g), thermal conductivity (k_g), emissivity (ϵ_g), and temperature of the PV glass layer (T_g).

In the second layer EVA1, the energy balance equations can be expressed by Eq. (29) as follows:

Energy balance equation for EVA1 layer:

$$\begin{aligned} Q_{in} &= Q_{out} \\ Q_{abs} + Q_{con c\to EVA1} &= Q_{con EVA1\to g} \\ \alpha_E G + \frac{k_E}{L_E}(T_c - T_{E1)} &= \frac{k_g}{L_g}(T_{E1} - T_{g)} \end{aligned} \tag{29}$$

where Q_{in} represents the energy input to the EVA1 layer, which includes the absorbed heat from by EVA1 ($\alpha_E G$) and the heat conducted from the PV cell layer $Qcon_{c\to EVA1}$. Meanwhile, Q_{out} represents the energy output from the EVA1 layer, the heat conducted to the PV glass layer. $Qcon_{EVA1\to g}$. Additionally, the properties of the EVA1 layer include absorption coefficient (α_E), thickness (L_E), thermal conductivity (k_E), and temperature of the PV cell (T_c).

For the PV cell layer, the energy balance equation can be expressed by Eq. (30) as follows:

$$\begin{aligned} Q_{in} &= Q_{out} \\ Q_{abs} &= Q_{\text{gen}} + Q_{con c\to E1} + Q_{con c\to E2} \\ \tau\alpha_c G = \tau\alpha_c G\eta_{PV} &+ \frac{k_E}{L_E}(T_c - T_{E1)} + \frac{k_E}{L_E}(T_c - T_{E2)} \\ \tau\alpha_c G(1 - \eta_{PV}) &= \frac{k_E}{L_E}(T_c - T_{E1)} + \frac{k_E}{L_E}(T_c - T_{E2)} \end{aligned} \tag{30}$$

Q_{in} represents the solar energy striking the PV cell layer, which is the absorbed heat from solar radiation ($\tau\alpha_c$ G) multiplied by the transmittance factor that accounts for the absorption or reflection of sunlight by the surface of preceding layers. Q_{out} represents the generated electrical power and the heat conducted to the EVA1 and EVA2 layers. Additionally, the properties of the PV cell include transmittance absorption coefficient ($\tau\alpha_c$), PV efficiency at working conditions (η_{PV}), which depends on the PV cell temperature as expressed in Eq. (31) [39].

$$\eta_{PV} = \eta_{ref}\,(1 - \beta(T_c - T_{a(ref)}) \tag{31}$$

where, η_{ref} is the PV efficiency at STC (1000 Wm^{-2}, 25 °C), β is the PV cell temperature coefficient [∘C^{-1}], and T_c is the PV cell temperature [∘C].

For the fourth layer EVA2, the energy balance equations can be expressed by Eq. (32) as follows:

Energy balance equation for EVA2 layer:

$$\begin{aligned} Q_{in} &= Q_{out} \\ Q_{con c\to EVA2} &= Q_{con EVA1\to bakc} \\ \frac{k_E}{L_E}(T_c - T_{E2)} &= \frac{k_b}{L_b}(T_{E2} - T_{b)} \end{aligned} \tag{32}$$

where, Q_{in} represents the energy input to the EVA2 layer, which is the heat conducted from the PV cell layer $Qcon_{c\to EVA2}$. Meanwhile, Q_{out} represents the energy output from the EVA2 layer, which is the heat conducted to the PV back layer (Tedler) $Qcon_{EVA2\to b}$. T_b is the back surface temperature of the PV module, and k_b and L_b denote the thermal conductivity and thickness, respectively, of the back surface of the PV module.

For the Tedlar layer (back surface of PV), the energy balance equation can be expressed by Eq. (33) as follows:

$$\begin{aligned} Q_{in} &= Q_{out} \\ Q_{con E\to b} &= Q_{conv} + Q_{rad} \\ \frac{k_b}{L_d}(T_{E2} - T_{b)} &= \text{hA}(T_b - T_a) + \epsilon_b\sigma A\left(T_b^4 - T_{sky}^4\right) \end{aligned} \tag{33}$$

where, Q_{in} represents the energy input to the Tedler layer, which is the heat conducted from the EVA2 layer $Qcon_{E2\to b}$. Q_{out} represents the energy output from the Back surface, which includes the heat loss to the atmosphere through convection ($Q_{conv} = Q_{convection}$) and radiation ($Q_{rad} = Q_{radiation}$). ϵ_b is the emissivity of the back layer of the PV module.

2.1.2.2. Dusty PV. The PV glass surface layer is primarily affected when dust accumulates on a PV module. The presence of dust on the module surface results in heat transfer through three main mechanisms [40]:

- Conduction: Heat is transferred between the PV module and dust particles and among the dust particles themselves.
- Convection: Heat is exchanged through convective heat transfer between the dust particles and the surrounding environment, as well as between the PV module and the surrounding environment.
- Radiation: Heat is radiated from the dust particles to other particles and from the particles to the sky. Additionally, heat is radiated from the PV module surface to the sky and the dust. Fig. 3 illustrates the different pathways of heat transfer.

However, due to the thermal equilibrium among dust particles and PV glass surface, the combined conduction and radiation heat transfer among dust particles can be neglected. Furthermore, because the dust particles are significantly smaller than the surface area of the PV module, radiant heat transfer does not occur, as the view factors between the particles and the PV surface are near zero bb. Therefore, this study will assume the primary impact is on the absorption of the glass surface. Consequently, the main distinction between dusty and clean PV modules lies in the glass layer, where the equation will be given in Eq. (34) as follows:

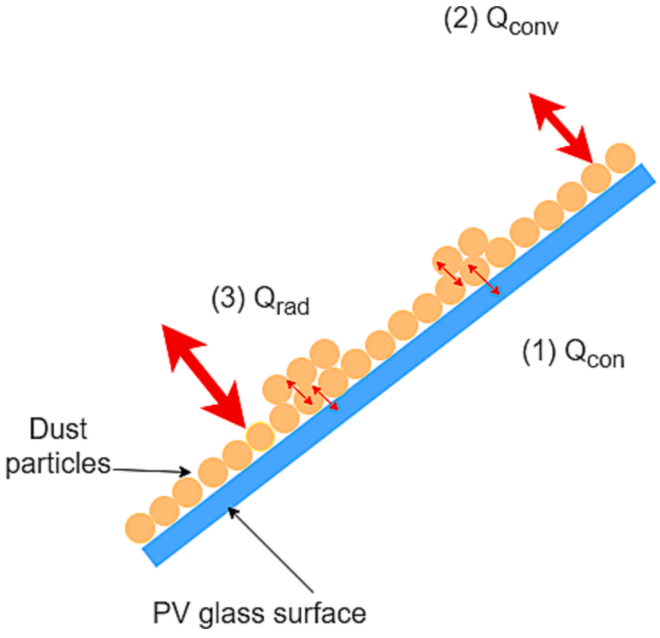

Fig. 3. Heat transport mechanisms in the dusty front side surface of the module - conduction (1), convection (2), and radiation (3).

$$Qin = Qout$$
$$Qabs(g+d) + Qcond = (Qcon + Qrad)$$
$$(\alpha g + \alpha d)G + \frac{k_g}{L_g}(T_{E1} - T_g) = \mathrm{h}(T_g - T_a) + \epsilon_{dg}\sigma\left(T_g^4 - T_{sky}^4\right) \quad (34)$$

Qin represents the energy input to the glass layer, including the heat absorbed by the glass and dust layer and the heat conducted from the second layer. Q_{out} represents the energy output from the glass layer, which includes heat loss via convection and radiation. Additionally, the properties of the dust layer include αd (absorption coefficient) and ϵ_{dg} (emissivity).

Considering these factors, this study assumes that the combined impact of dust accumulation primarily affects the absorption on the glass surface, which is the primary reason for the increase in the PV surface temperature. As the dust settles on the PV module surface, it reduces the transmittance of solar radiation through the glass, resulting in higher absorption of solar energy by the dusty module. This increased absorption leads to an elevation in the PV surface temperature, impacting the overall performance and efficiency of the PV module.

Therefore, the flowchart in Fig. 4 illustrates the equations used to calculate the impact of dust on PV temperature, along with the primary devices required to measure the dust parameters. These devices have been employed to replicate real-world conditions and ensure accurate calculations. The flowchart outlines the step-by-step process of accounting for dust effects on PV temperature, considering the altered transmittance and absorption on the glass surface due to dust accumulation. By utilising the measured dust parameters and applying the derived equations, valuable insights are gained into the PV module's actual temperature rise and performance changes under dusty conditions.

The calculation equations will integrate additional pertinent values and parameters from Table 2, which includes parameter values obtained from published work. These parameters encompass thermal conductivity (k), thickness (L), transmittance, and absorption coefficients for clean PV materials, all of which are crucial for precise assessments. However, to accurately estimate the behaviour of the dusty PV module, further investigation will be necessary to ascertain the parameters specific to dusty conditions. This meticulous approach guarantees a more accurate

Table 2
Properties of different layers in PV modules [41,42].

No	Layer	Properties			
		Length L (mm)	*Thermal conductivity k* ($Wm^{-1}K^{-1}$)	Emissivity	Absorptivity
1	Glass	3	0.9	0.88	0.2
2	EVA1,2	0.5	0.35		0.02
3	PV cell	0.3	148		0.85
5	PV back	0.1	0.2	0.87	0.5

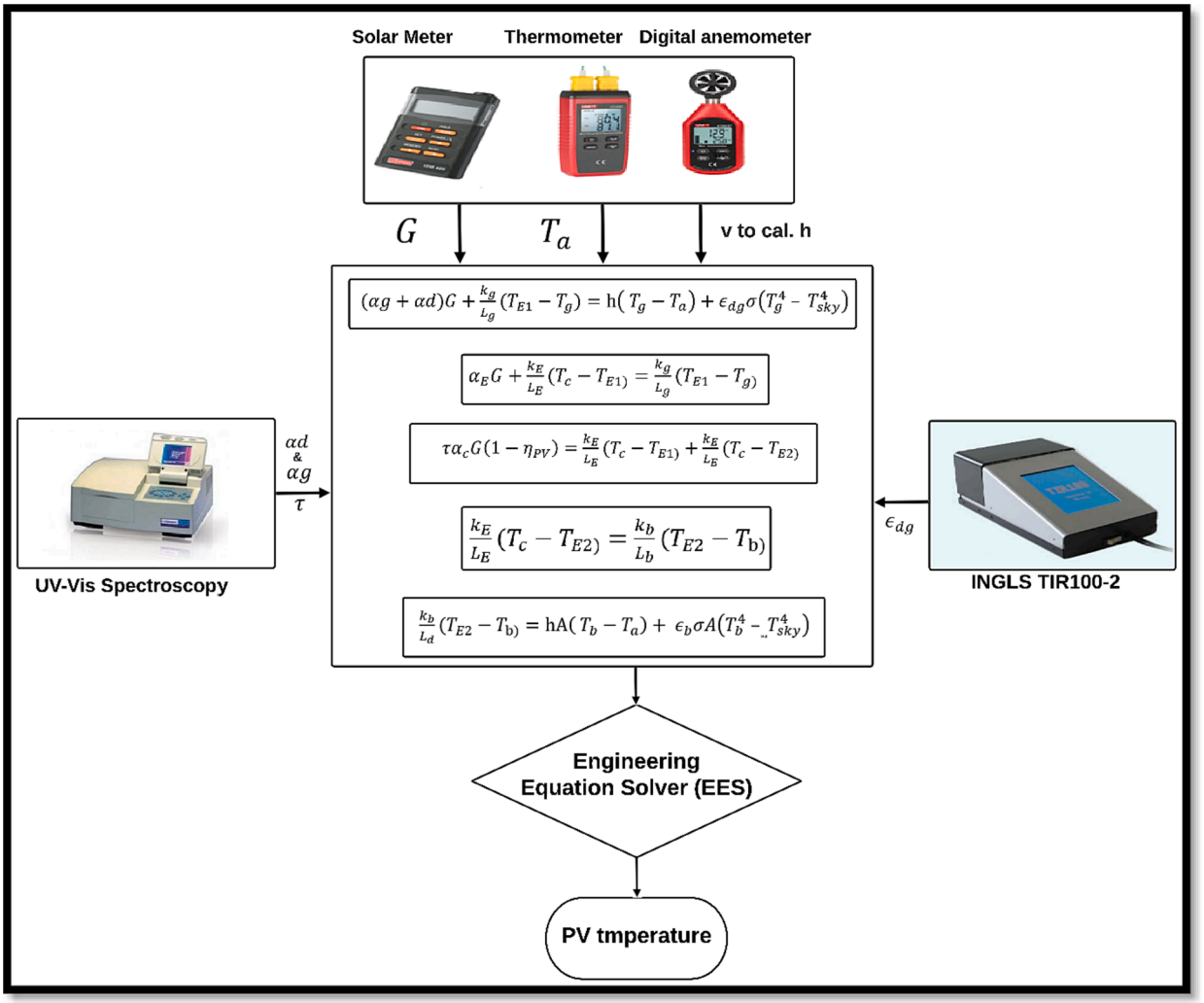

Fig. 4. Flowchart for estimating the impact of dust on PV temperature.

and realistic estimation of the impact of dust on the PV module's behaviour, facilitating a comprehensive analysis and dependable results.

2.2 Study location and experimental setup

Dust phenomena fall under the category of dry climatic events originating from the thermal heating of the air near the Earth's surface [43]. These phenomena are especially prevalent in arid and semi-arid locations, such as the Middle East and North Africa [44]. Given the ideal conditions in these areas for studying the effects of dust on PV modules, this research is concentrated on data collection in Iraq. Iraq is characterized by high ambient temperatures, intense solar radiation, and frequent dust storms resulting in substantial dust accumulation. This unique combination of factors makes Iraq an apt location for investigating the impact of dust on PV module temperature.

For this study, dust samples were collected from two distinct regional dust storms in Iraq. By obtaining dust samples from these regional dust storms, the research aims to analyse the collected dust's characteristics and composition and investigate their influence on the temperature and performance of PV modules. This data collection approach enables a comprehensive examination of the variations in dust properties and their potential impact on PV systems in Iraq.

2.2.1. Dust collection procedure

The experimental setup involved strategically placing a large 4 × 4 m plastic sheet outdoors to capture dust during regional dust storms. When a dust storm occurred, the wind transported dust particles that settled and accumulated on the sheet. This method facilitated the collection of dust samples from multiple dust storms, enabling a comparative analysis of their characteristics and effects. The sheet remained in position throughout the dust storm to capture a representative sample of the deposited dust. Once the dust storm subsided, the plastic sheet with the accumulated dust was carefully gathered to preserve the sample's integrity.

The collected dust samples were stored in a controlled environment to prevent any alteration of their properties. Subsequently, the collected dust samples underwent various analyses, including physical and chemical characterisation, to determine properties such as particle size, shape, chemical composition, emissivity, transmittance, and absorption. These analyses provided a comprehensive understanding of the dust samples' characteristics and their potential effects on the performance of PV modules. By employing this collection method and conducting a thorough analysis, the study aimed to gain insights into the variations in dust composition and characteristics, enhancing the understanding of the impact of dust on PV module temperature and performance.

2.2.2. Dust characterization

The fundamental properties of the collected dust samples were investigated to gain a comprehensive understanding of their characteristics.

2.2.2.1. Chemical parameters of dust. X-ray fluorescence (XRF) analysis was utilised to examine the chemical composition of the gathered dust samples. This analytical technique entailed subjecting the dust particles to X-rays, inducing them to emit distinctive fluorescent X-rays. Subsequently, the emitted X-rays were measured and scrutinised to ascertain the elemental composition of the dust samples. The XRF analysis yielded valuable insights into the presence and concentration of various elements within the dust.

2.2.2.2. The emissivity of the dusty PV surface. The emissivity of the dusty PV surface was determined using the thermal emissivity measuring device (INGLAS TIR100-2), as depicted in Fig. 5. Prior to conducting the measurements, the instrument underwent preheating over an hour to ensure temperature stability. Calibration of the instrument was achieved using two reference surfaces with known emissivity values: white and black surfaces. Subsequently, the collected dust samples were uniformly distributed on the PV surface, and emissivity measurements were recorded. This procedure was repeated for varying amounts of dust and samples from different dust storms, enabling the capture of a broad spectrum of emissivity values.

2.2.2.3. Optical properties of the dusty PV surface. Small glass sheets (25.4 × 76.2 mm) were coated with the collected dust particles to examine the transmittance and absorption characteristics of the dust, as illustrated in Fig. 6. These dust-coated glass sheets underwent analysis using UV–vis Spectroscopy Instrumentation following established standards. The UV–vis Spectroscopy analysis offered insights into the transmittance and absorption properties of the dust samples, facilitating a deeper comprehension of their optical influence on PV systems.

All experiments, including XRF analysis, emissivity measurements, and transmittance and absorption analysis, were conducted by established standard methods in a specialized laboratory.

2.3. Outdoor experimental setup

The outdoor experiments were conducted in Baghdad, Iraq, under outdoor conditions to replicate real weather conditions.

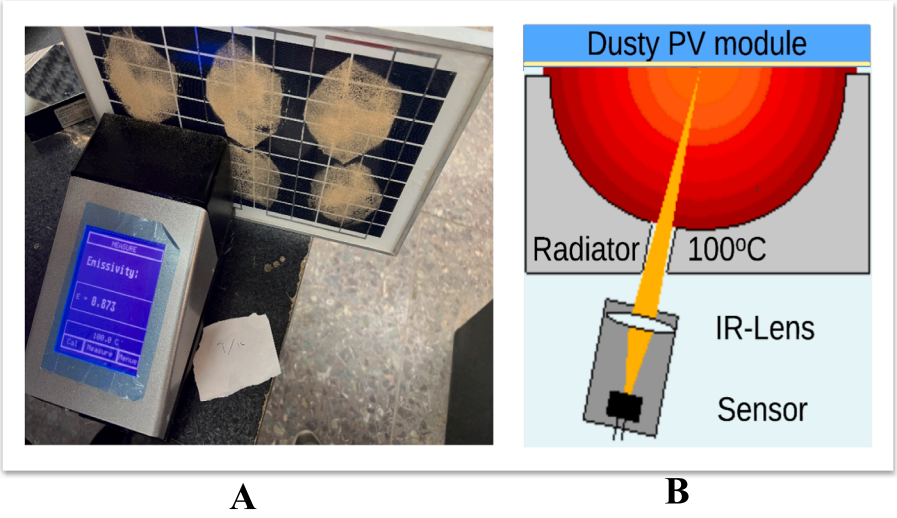

Fig. 5. Demonstrates dusty PV emissivity measurement. B: emissivity measurement principle for the tir100-2. A: photographic representation of the device.

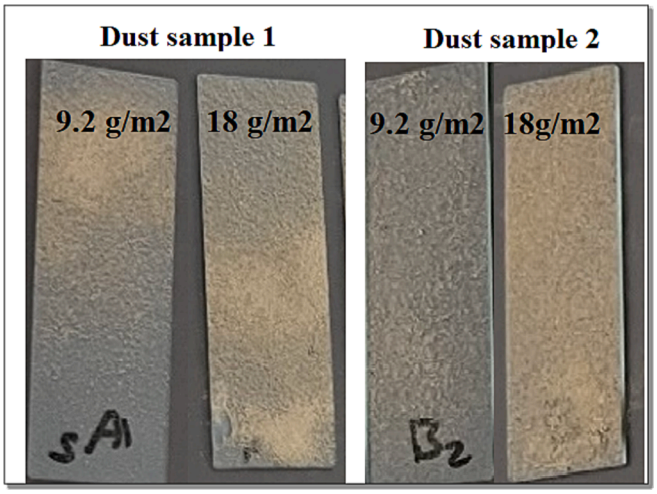

Fig. 6. Glass sheets coated with the collected dust for sample 1 and 2.

An outdoor experiment involved the utilisation of three identical PV modules with specific technical specifications, as detailed in Table 3. Each module served a specific purpose:

- Reference Panel: A clean PV module was utilised as the control group to establish baseline performance.
- PV Module 2: The PV module is exposed to a specific type and quantity of dust to simulate real-world environmental conditions.
- PV Module 3: Exposed to a different type of dust with the same quantity to provide data concerning the influence of diverse dust compositions.

All three PV modules were affixed to a custom-built frame, ensuring that they were aligned in the same orientation and tilt angle for consistent measurements. The orientation was adjusted to guarantee direct sunlight exposure, and the tilt angle was regularly modified to maintain optimal solar energy absorption.

During the outdoor experiments, the following parameters were consistently measured and recorded:

- Temperature Data: Ambient temperature was monitored using thermal couples to record the environmental temperature, while thermal cameras were employed to measure the temperature of each PV module at regular intervals.
- Solar Radiation: Solar irradiance incident on the PV modules was documented using pyranometers.
- Other Environmental Factors: Additional environmental factors, such as wind speed, were measured using a wind speed meter.

Table 3
The PV module's technical specifications.

Maximum power at STC (*Pmax*)	10 (W)	Cell type	Monocrystalline
The voltage at the maximum power point (*Vmp*)	17.6 (V)	N. cell	36
Current at the maximum power point (*Imp*)	0.57 (A)	Dimensions	320 × 350 (mm)
Open circuit voltage (*Voc*)	21.6 (V)	Weight	1 kg
Short circuit current (*Isc*)	0.62 (A)	Power temperature coefficient	−0.36 %/°C2
NOCT	45 °C	Power measurement tolerance	−0.03

- The Solar Module Analyzer was utilised to assess the performance and output of each PV module, providing valuable data on efficiency and power generation under varying dust conditions.

Fig. 7 illustrates the outdoor experiment setup, depicting the positioning of three identical PV modules, the custom-built frame, and the array of measurement tools employed for data collection during the study. The instruments and devices utilised for data collection in the outdoor experiment are detailed in Table 4, which provides information about the equipment's make, model, accuracy, and measuring ranges, including pyranometers, thermal cameras, wind speed meters, and the solar module analyzer.

To gain a comprehensive understanding of the effects of dust accumulation on PV modules, two sets of experiments were conducted to investigate the impact of both the quantity and composition of dust on PV temperature and performance. To align the study with real-world conditions, dust samples were collected from two regional dust storm events that occurred in Middle Eastern countries on May 13 and May 23, 2022. These samples, identified as "Dust Sample 1" and "Dust Sample 2," directly represent actual environmental conditions. Two different dust amounts were considered: 9.2 and 18 g/m^2. The experimental data has been organized in Table 5 for ease of reference and to maintain clarity.

The outdoor experiments were conducted during the summer season and on a hot day, precisely from 11:30 a.m. to 1:30 p.m. This timeframe was chosen to precisely assess the impacts of varying dust levels and compositions on the temperature and performance of the PV modules. It also enabled the observation of variations in environmental conditions and seasonal changes that might affect the PV modules' performance. The experiments were repeated multiple times to ensure the reliability and validity of the results. Each replication was conducted under similar conditions, ensuring consistency in the setup and data collection procedures.

3. Result and discussion

The study's results and discussion section have been divided into three main categories. Firstly, the dust properties are presented. This section includes the results obtained from laboratory tests conducted by specialists to measure dust properties, such as transmittance, absorptance, emissivity, and the chemical composition of the dust.

Secondly, the outcomes of the theoretical model have been compared with the outdoor results to determine the accuracy of the proposed mathematical model.

Finally, the outdoor results have been presented and analysed. This section encompasses the experiments' results obtained from three PV modules installed outdoors under realistic weather conditions, including PV module temperature performance.

In each of these categories, a detailed analysis and discussion of the results are provided to offer a comprehensive understanding of the impact of dust on PV performance.

3.1 Characteristics and chemical composition of the dust sample

The dust samples used in this study were collected during Iraq's regional dust storms on the 13th and 23rd of May 2022. The investigation aimed to understand the chemical and optical properties of dust and their influence on PV temperature.

3.1.1. Chemical analysis

To elucidate the chemical composition of the dust samples, the XRD method was employed. The results from this analysis are visualized in Fig. 8, which depicts the XRF scan showing the proportion of various elements in each dust type. A comprehensive breakdown of the chemical composition is provided in Table 6. Notably, the results highlight the presence of significant components, including Si, Al, Fe, Ca, Mg, S, and

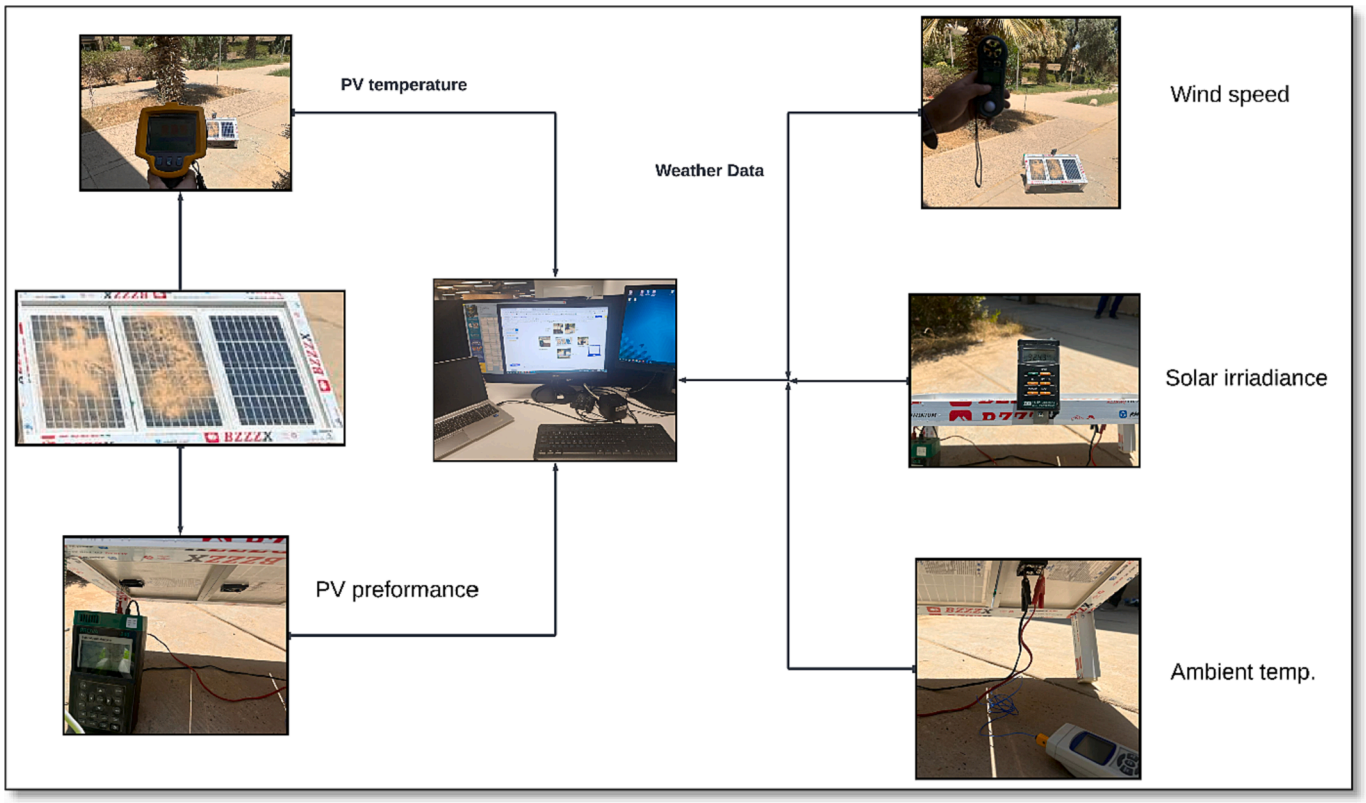

Fig. 7. Illustrates the arrangement of the outdoor experiment with the three identical PV modules.

Table 4
Instrument device and specification used in the outdoor experiment.

Experimental equipment	Manufacturer and model	Measurement error
Pyranometers	RS PRO Solar Power Meter ISM400	±10 W/m^2
Thermometer	Uni-T UT320D	± (0.5 % + 1)
Solar module analyzer	PROVA 200	±1%
Digital anemometer	UNI-T UT363	± 0.1 m/s
Thermal camera	Fluke Ti10	±2°C

Table 5
Experimental test samples.

Test set	Dust sample	Dust weight (g/m^2)
Test set 1	Dust sample 1	18
	Dust sample 2	18
Test set 2	Dust sample 1	9.2
	Dust sample 2	9.2

K, among others. The proportions of these elements are detailed below. These findings played a pivotal role in comprehending material properties and their influence on PV performance, with slight observation between the two samples.

3.2 The optical characteristics

The optical characteristics of the dust samples held significant importance in this study, given their crucial role in understanding developing an accurate model for assessing the impact of dust on PV temperature. Precise measurements and analyses were conducted to investigate the dust samples' transmittance, absorption, and emissivity properties. This rigorous approach was taken to ensure the reliability and validity of the developed model, emphasizing the importance of employing accurate data rather than estimated values.

Figs. 9 and 10 illustrate the transmittance and absorbance results obtained from the UV–vis Spectroscopy for two different types and two different weights of dust (dust sample 1 (dust 1), dust sample 2 (dust 2)). These graphs depict variations in transmittance and absorption attributable to dust type and weight. The data analysis allows for a deeper understanding of how different dust compositions and densities affect light transmission and absorption through the samples. These measured values serve as crucial inputs for the proposed model, enabling the accuracy of the assessment of the dust's effects on PV modules.

3.2.1. The emissivity of PV module

Emissivity, another critical optical property, was examined in the laboratory experiments using the INGLAS TIR100-2 Thermal emissivity measuring instrument, as described in the methodology Section above. Emissivity plays a significant role in determining the radiative heat transfer characteristics of PV surfaces covered with dust. The measured emissivity data for different dust types and densities are presented in Table 7.

The optical results, summarized in Table 7, offer valuable insights into the potential impact of different dust types on various applications and systems. This table highlights the optical properties of the dust, essential for refining the calculations of the developed equations and accurately assessing the effects of dust on PV temperature.

A comprehensive understanding dust's complex chemical and optical properties is essential for refining the calculations of the developed equations and accurately assessing the effects of dust on PV temperature.

The observed trends in the optical properties provide insights into the behaviour of dust-covered surfaces and their influence on PV performance. As the amount of dust increased, the transmittance decreased, highlighting the obstructive nature of higher dust densities. Conversely, absorption and emissivity values increased with higher dust density, indicating greater light interaction and heat radiation. These

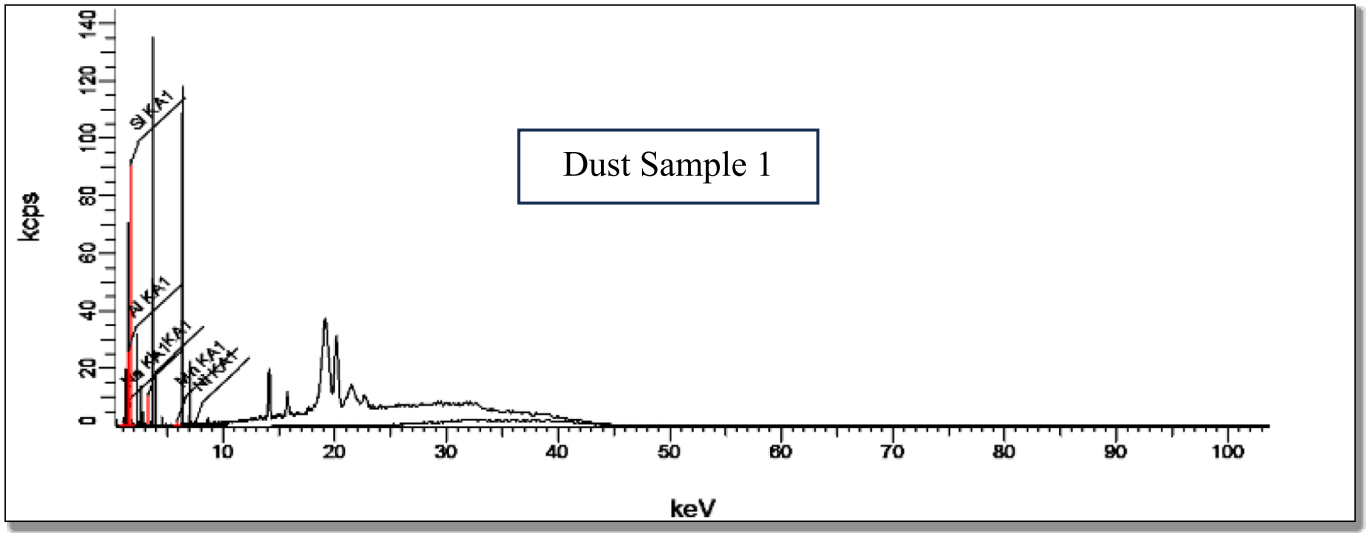

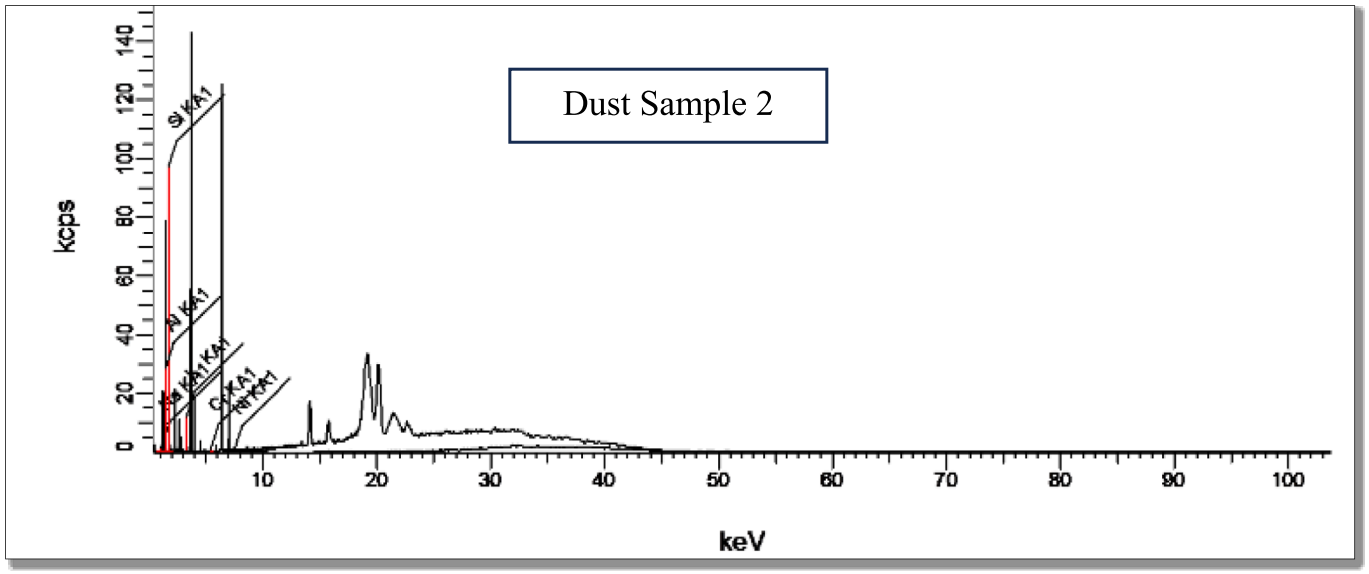

Fig. 8. The XRF Scan shows the proportion of various elements and materials in each dust type.

Table 6
The proportion of various elements and materials present in each dust type.

Element	Dust Sample 1 (13-May)	Dust Sample 2 (23-May)
Si (%)	30.31	31.35
Al (%)	9.27	9.80
Fe (%)	9.49	9.70
Ca (%)	34.78	34.80
Mg (%)	5.01	5.01
S (%)	5.47	3.50
K (%)	2.69	2.82

fluctuations in optical properties underscore the significance of using accurate data to estimate the impact of dust on PV temperature.

When comparing different dust types, slight variations in the optical property values were observed, attributed to the distinct compositions and sizes of dust particles in each sample. Variations in chemical composition can alter the optical properties, affecting scattering and absorption characteristics, while differences in particle size can further influence the optical behavior of the dust samples. Understanding these variations is crucial for accurately modeling the impact of specific dust types on PV modules. These intricacies in dust properties lead us to the next phase of our study, focusing on real-world implications.

3.2.2. *Outdoor results*

Building upon the insights gained from the analysis of dust properties, the primary objective of the outdoor experiments was to validate the developed mathematical calculations for estimating PV temperature under dusty conditions. Three PV modules were used: one was kept clean, while the other two were exposed to different dust compositions, weighing 0.9 g and 1.8 g, respectively.

Fig. 11 illustrates thermal imaging conducted using the thermal camera, as detailed in the methodology section. This visualization provides a comprehensive understanding of the temperature distribution across the PV modules. The thermal images vividly demonstrate a correlation between the dust accumulation on the PV modules and elevated PV cell temperatures. As shown in Fig. 11, distinct temperature points are indicated with accompanying temperature readings. This temperature fluctuation is crucial for comprehending how the PV modules respond to varying dust levels and how this interaction impacts their thermal behaviour.

The PV analyser (PROVO 2000) evaluated the electrical performance

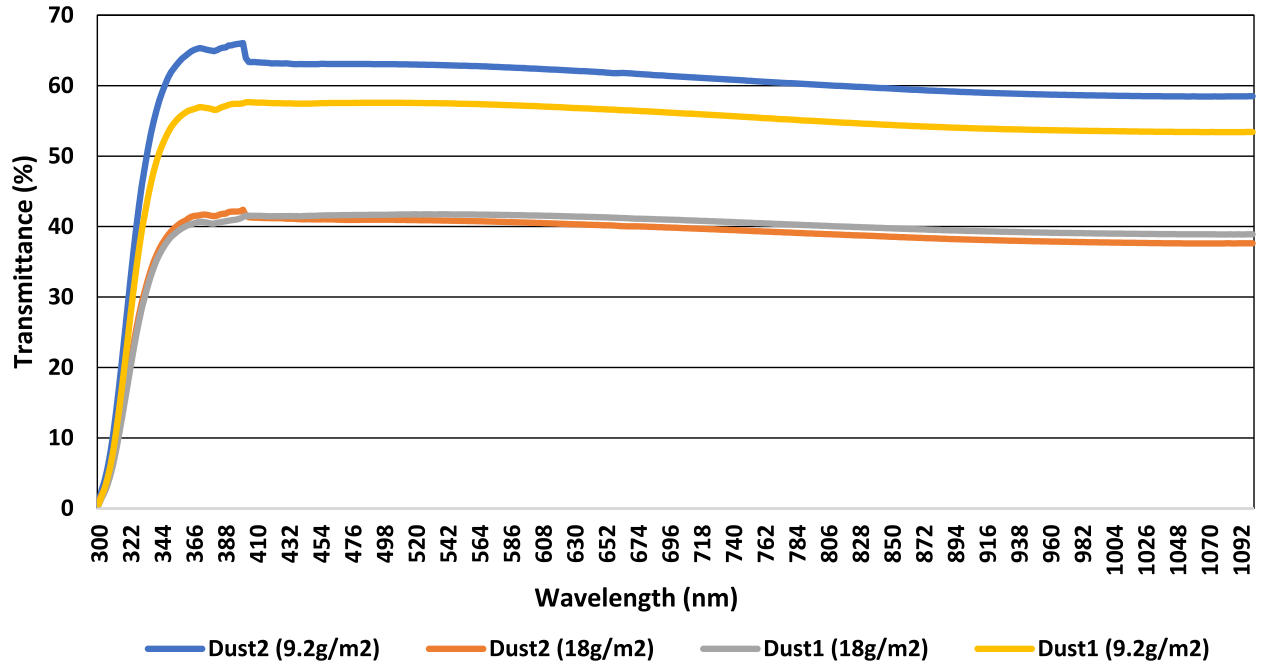

Fig. 9. Transmittance trends of different dust types and amounts.

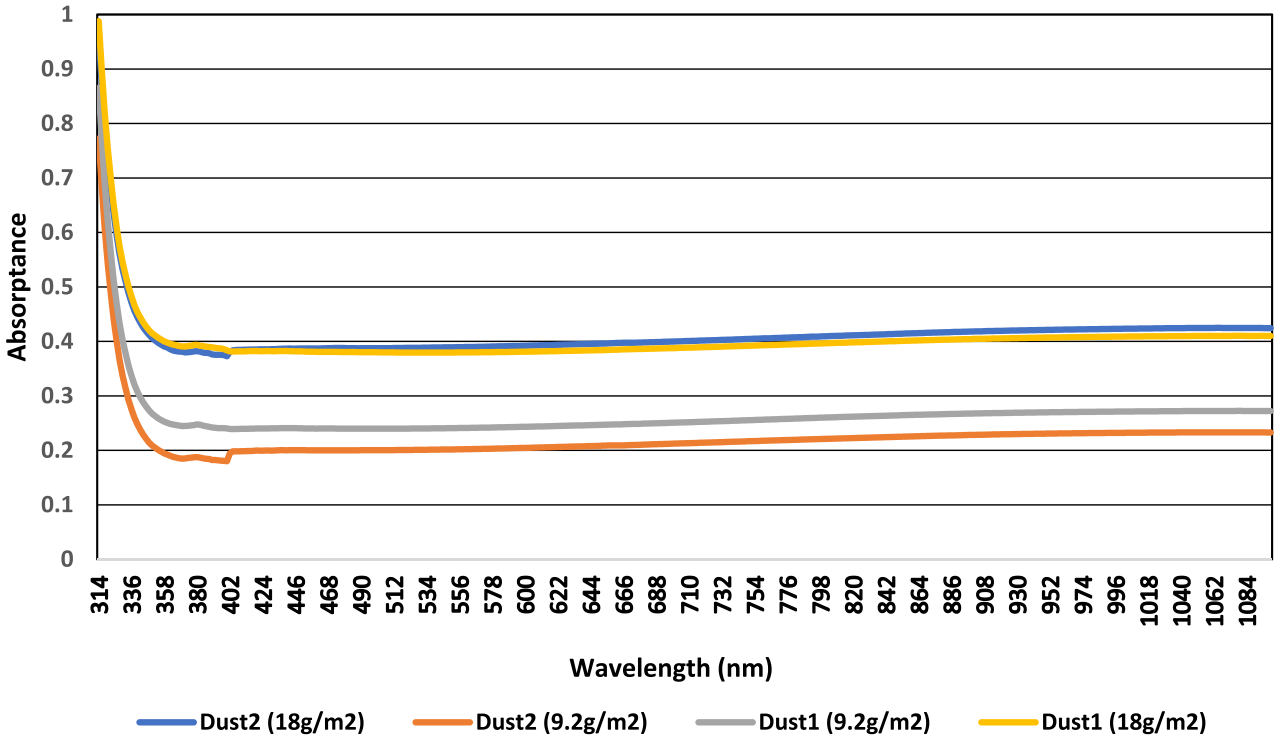

Fig. 10. Absorption trends of different dust types and amounts.

Table 7
Dust sample optical properties: changes in optical properties with varying dust densities and chemical compositions.

Dust type	Transmittance		Absorptance		Emissivity	
	9.2 g/m^2	18 g/m^2	9.2 g/m^2	18 g/m^2	9.2 g/m^2	18 g/m^2
Dust 1	56 %)	41 %	0.25	0.39	0.871	0.886
Dust 2	62 %	40 %	0.21	0.4	0.889	0.902

of the PV modules. Fig. 12 presents the I-V characteristics of the clean and dusty PV modules. The clean PV module exhibited the expected V-I curve (Fig. 11A). In contrast, the dusty PV modules exhibited deviations (Fig. 11B) attributed to the impact of dust on the module's optical properties, which influenced its efficiency and electrical output.

The analysis revealed a significant impact on PV current due to the reduced incident light intensity reaching the PV cell. However, the effect on PV voltage was relatively minor, as dust accumulation mainly influenced the optical properties of the light-absorbing layer. Overall,

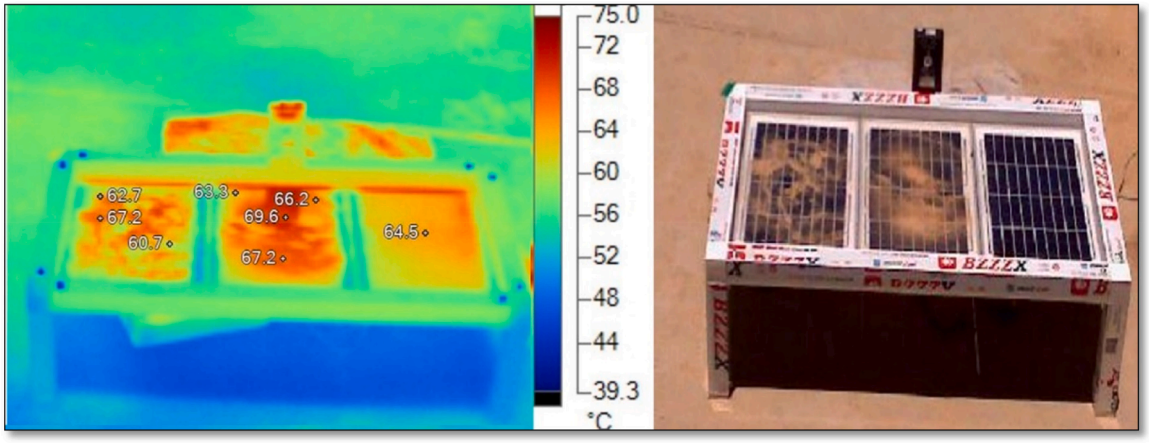

Fig. 11. Thermal Imaging Comparison (A) Thermal imaging captured using a thermal camera, highlighting temperature variations. (B) Visible image.

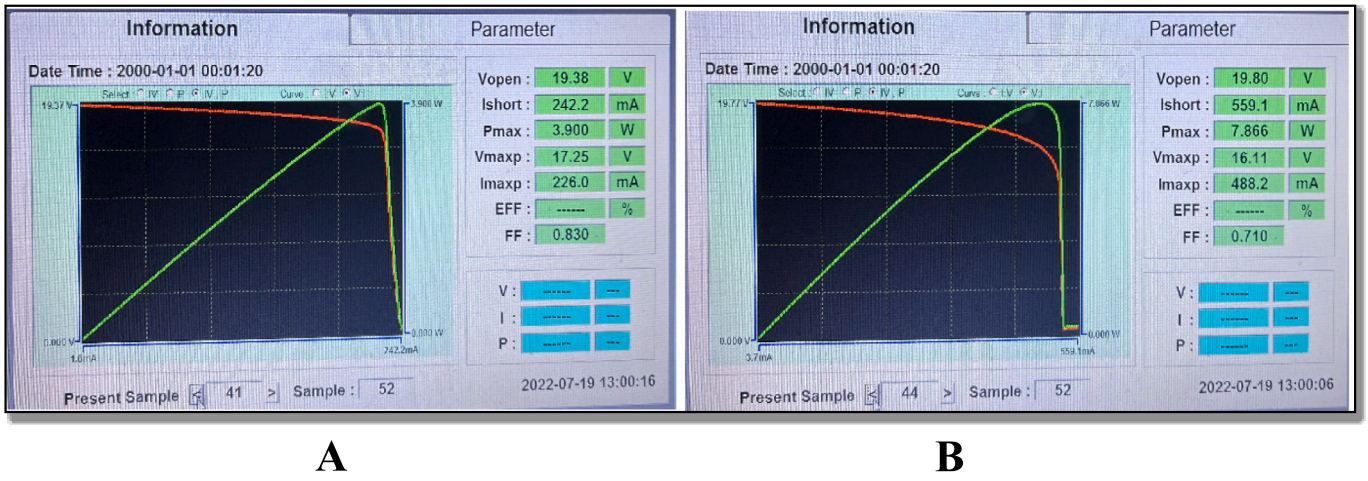

Fig. 12. V-I (Voltage-Current) Characteristics of PV Modules: (A) V-I of a Dusty PV Module, and (B) V-I of a Clean PV Module.

the dusty PV modules experienced considerably lower electrical power output.

In addition to temperature data, the outdoor experiments collected other crucial atmospheric environment parameters using the mentioned devices. These parameters, including solar irradiance (G), wind speed (V), and ambient temperature (T_a), are vital for developing accurate calculations and validating the developed models. Table 8 presents a comprehensive set of these parameters alongside the electrical and temperature measurements of the clean and dusty PV panels. Combining these atmospheric parameters with the temperature data enables a more thorough analysis of the impact of dust on PV performance under varying environmental conditions.

These findings underscore the effects of dust on PV systems and emphasise how different dust compositions and weights directly influence PV cell temperature and electrical output power. The data from the outdoor experiments offer conclusive evidence of the substantial impact of dust on PV temperature and performance, prompting a deeper dive into the theoretical framework that governs these interactions. The rise in PV cell temperature and the variations in electrical characteristics due to dust accumulation highlight the importance of precise estimations of PV temperature and other atmospheric parameters.

3.3. Simulation results

In light of the empirical evidence obtained from the outdoor experiments, the study employed an iterative solution process facilitated by

Table 8
Outdoor data results for weather conditions, PV temperature, and output power for the clean and dusty PVs.

		Weather data			Clean PV		Dusty sample 1		Dusty sample 2	
	Time	Solar irradiance G (w/m^2)	Wind speed v (m/s$^{2)}$	Ambient temperature T_a (^{o}C)	T_{PV} (^{o}C)	Power (W)	T_{PV} (^{o}C)	Power (W)	T_{PV} (^{o}C)	Power (W)
Test 1	10:20	910	0.5	44.0	67.50	7.46	68.2	3.78	66.8	3.21
18 g/m^2	10:40	930	1.2	44.8	63.80	7.80	66.8	3.86	66.2	3.24
	10:50	930	1.0	45.0	63.00	7.95	66.8	3.90	65.3	3.28
Test 2	11:30	950	0.5	45.7	64.5	7.49	69.6	4.43	67.2	4.92
9 g/m^2	11:50	938	0.5	47.5	66.00	7.61	70.3	4.23	68.8	4.89

the Engineering Equation Solver (EES) software to effectively address the complex thermal dynamics of a multi-layered PV module under changing weather conditions. The entire process can be summarised in a flowchart that outlines the sequential steps to achieve the desired results, as depicted in Fig. 13.

The flowchart emphasises the iterative solution process enabled by the EES software for solving a complex equation system. It specifically addresses the intricate thermal dynamics of a multi-layered PV module under varying weather conditions. The process commences with the initialisation of variables and the establishment of initial temperature estimates. Through iterative cycles, EES computes temperature-dependent properties and heat transfer coefficients among the layers. Net heat transfer rates are then analysed, and variables are updated using energy balances and layer-specific equations. A convergence check, which measures the disparities between current and previous values, guides the process. Revised estimates are employed if convergence is not achieved, sustaining the iterative loop until the defined convergence criterion is met. Upon satisfaction of this criterion, the loop concludes, yielding a set of reliably estimated PV layer temperatures that constitute the solution. EES orchestrates this complex process by integrating weather data, properties of the PV material, and experimental details to achieve a dependable and effective solution for the equations. These solutions then needed empirical validation to confirm their accuracy and reliability.

3.4. Validation of mathematical model

Following the derivation of the theoretical solutions, the validation process entailed comparing the predictions of the mathematical model with the outcomes obtained from the outdoor experiments conducted under real-world weather conditions. The temperatures listed in Table 9 correspond to measurements taken for PV modules in various scenarios. To further assess the accuracy of the developed equation, the Mean Absolute Error (MAE) method was employed - a dependable metric for evaluating predictive precision. Eq. (35) computes the MAE, facilitating a comparison between the developed equation and experimental results.

$$MAE = \frac{1}{n}\sum_{i=1}^{n}\left|T_{predicted} - T_{observed}\right| \tag{35}$$

Table 9 presents a comparison between the model's predictions with the corresponding experimental results. The assessment of the model predictions and the outdoor experimental data demonstrated a close agreement, with MAE of 7.2 and 1.46, respectively. This validation confirms the model's efficacy in capturing the impact of dust on PV temperature. The theoretical calculations closely aligned with the experimental results, affirming the reliability and consistency of the developed equations. To further emphasise the reliability of the developed model, it was pivotal to compare it against existing equations in the literature.

3.5 Comparison with established equations

Having validated the accuracy and effectiveness of our developed correlation equation, it was subjected to further scrutiny through a comprehensive comparative analysis with established equations for estimating PV temperature in dusty environments. This evaluation assessed the equation's performance by contrasting it with previously established mathematical models. To ensure a thorough assessment, the developed equation was compared with Eqs. (18)–(23) from the existing literature. This subset of equations was selected for their incorporation of optical properties and consideration of the reduction in light transmission resulting from dust accumulation. The comparison involved both actual PV temperature data collected from the author's outdoor experiments and the calculated values using the developed equations and the eight selected equations (Eqs. (18)–(23)) designated for

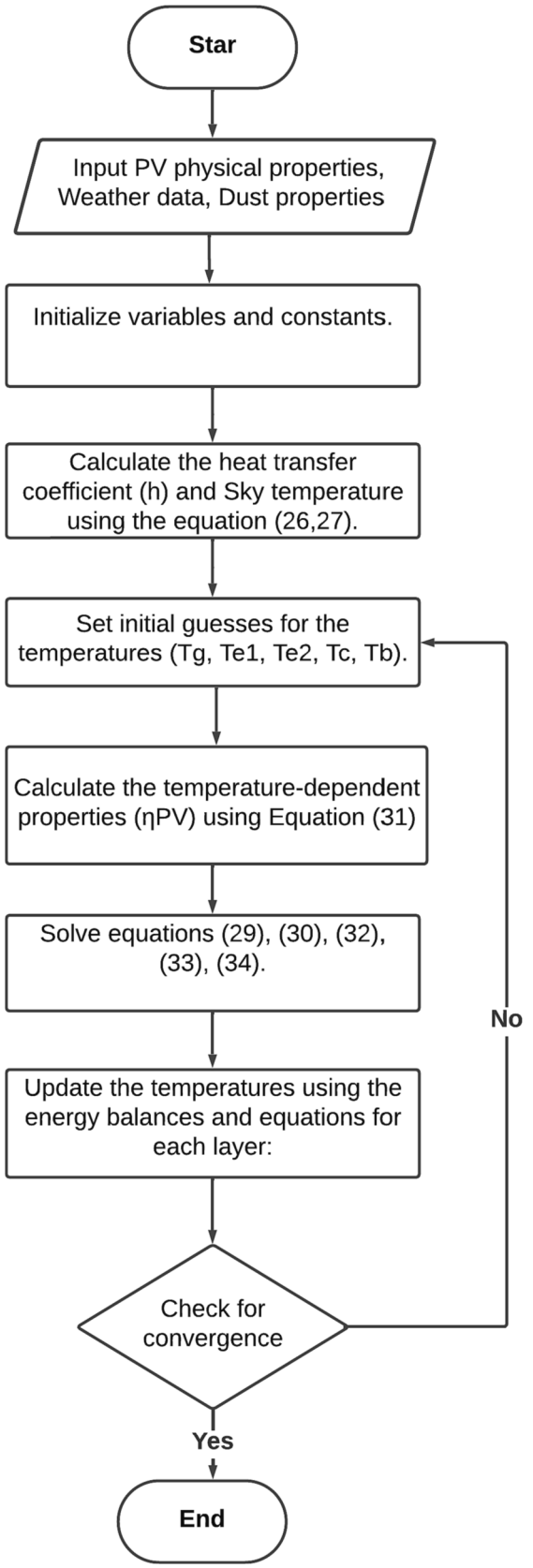

Fig. 13. Solution process for analysing multi-layered photovoltaic module thermal dynamics using EES software.

Table 9
The compression results of the experimental, new simplified, and five-layer developed models, and the MEA.

	T_{PV} (°C) (Experimental data)	T_{PV} (°C) (Simplified model)	T_{PV} (°C) (Five layers model)
Clean PV	67.5	59.0	63.68
	63.8	59.1	63.48
	63.0	59.6	64.08
Dusty 1 (18 g/m²)	68.2	58.6	65.20
	66.8	58.8	65.00
	66.8	59.3	65.60
Dusty1 (9.2 g/m²)	69.6	60.6	67.10
	70.3	62.4	68.60
Dusty 2 (18 g/m²)	66.8	58.6	65.30
	66.2	58.8	65.00
	65.3	59.3	65.60
Dusty 2 (9.2 g/m²)	67.2	60.6	67.00
	68.8	62.4	68.50
MAE		7.17	1.46

comparison, as presented in Table 10. This comprehensive evaluation underscores the importance of accounting for dust parameters to achieve accurate prediction of PV temperature.

The performance of Eqs. (18)–(23) in predicting dusty PV temperature in dusty conditions is visualised in Fig. 14. This clustered chart displays the MAE values, making it easy to compare their performance across different experiments. Notably, Eqs. (18)–(23) exhibit strong predictive capabilities, but it's worth noting that the developed equation consistently outperforms all others. The results of the comparative evaluation clearly underscore the superior accuracy of the developed equation. While Eqs. (21) and (22) achieve good predictions for clean surfaces, their accuracy diminishes for dusty surfaces. In contrast, the new simplified and five-layer equations for PV surfaces demonstrate enhanced accuracy, with MAEs of 7.1 and 1.4, respectively.

The accuracy of the developed equation makes it an excellent tool for estimating PV temperature while accounting for the sensitive interaction between optical and thermal properties on dusty PV surfaces. The study's findings emphasise the importance of including dust parameters for precise temperature estimations.

4. Conclusion

In conclusion, this study provides a comprehensive exploration of the intricate relationship between dust accumulation and PV module systems. Through systematic experimental analysis and advanced mathematical modeling, the research reveals the significant impact of dust on PV temperature and efficiency. Employing experimental techniques, critical optical properties such as transmittance, absorbance, and emissivity are quantitatively examined, shedding light on their crucial role in influencing heat transfer within the PV modules.

The outdoor experiments emphasise elevated PV cell temperatures and diminished electrical output power in dusty PV systems, highlighting the urgent need for accurate PV temperature estimation in dusty environments. The developed mathematical models, both the simplified one and the one consisting of five derived equations solved by the EES program, can accurately predict PV temperatures across different surfaces with MAEs of 7.1 and 1.4 respectively. Validation against experimental data verifies its precision in capturing the nuanced influences of dust on PV temperature.

Furthermore, this study extends to a comparative evaluation of established equations, encompassing optical properties and dust-related effects. The developed mathematical model emerges as a superior predictor of PV temperature in dusty conditions, exhibiting the lowest MAE. This research contributes to a deeper understanding of the intricate interplay between dust accumulation and PV module performance. It paves the way for future innovations in the field by providing a robust framework for analyzing the impacts of dust on PV modules. By integrating dust parameters and optical properties, the findings hold profound practical implications for accurately estimating PV temperature, enhancing efficiency, and ensuring reliability in dusty environments.

In light of the findings, the study asserts the significance of delving deeper into the multifaceted impacts of dust accumulation, and it encourages the exploration of adaptive strategies and advanced materials to mitigate the adverse effects of dust on PV modules.

Prospects:

1. Future research should focus on the intertwined effects of dust accumulation and high-temperature environments on the long-term degradation of PV modules.
2. Understanding these combined effects can guide the development of superior materials and designs that ensure PV modules retain their efficiency over extended periods, even in harsh conditions.
3. Investigations into how dust and temperature extremes impact PV module lifespans can inform more effective maintenance practices, leading to improved durability and performance.
4. Research into the combined impacts of dust accumulation and extreme temperatures can yield insights into potential weakness and pave the way for innovative module designs.
5. Continued exploration of advanced materials that resist the adverse effects of dust accumulation will be pivotal in enhancing the efficiency and longevity of PV modules in dusty environments.

This underscores the pressing need for collaborative efforts and interdisciplinary research to advance the field of solar energy and address the challenges posed by environmental conditions.

Declaration of Competing Interest

The authors declare that they have no known competing financial interests or personal relationships that could have appeared to influence

Table 10
PV temperature in degrees Celsius (°C) from experiments, developed and published equations.

	Experiment	Simplified model	Five layers model	Eq. (18)	Eq. (19)	Eq. (20)	Eq. (21)	Eq. (22)	Eq. (23)
Clean PV	67.5	59.0	63.68	67.7	69.7	68.4	68.2	67.7	65.3
	63.8	59.1	63.48	69.0	69.7	66.2	65.6	65.3	65.4
	63.0	59.6	64.08	69.2	70.3	67.3	66.9	66.5	65.9
Dusty 1 18 g/m²	68.2	58.6	65.20	54.3	55.1	48.8	46.3	46.4	44.0
	66.8	58.8	65.00	55.3	55.6	49.0	44.5	44.6	44.8
	66.8	59.3	65.60	55.5	56.0	49.4	45.4	45.5	45.0
Dusty 1 9.2 g/m²	69.6	60.6	67.10	52.6	53.2	50.1	47.5	47.5	45.0
	70.3	62.4	68.60	54.3	54.9	51.9	49.4	49.4	46.8
Dusty 2 18 g/m²	66.8	58.6	65.30	54.5	55.4	48.8	46.3	46.4	44.0
	66.2	58.8	65.00	55.6	55.9	49.0	44.5	44.7	44.8
	65.3	59.3	65.60	55.8	56.2	49.4	45.5	45.6	45.0
Dusty 2 9.2 g/m²	67.2	60.6	67.00	51.5	52.0	49.8	47.1	47.2	44.7
	68.8	62.4	68.50	53.2	53.7	51.5	49.0	49.1	46.5

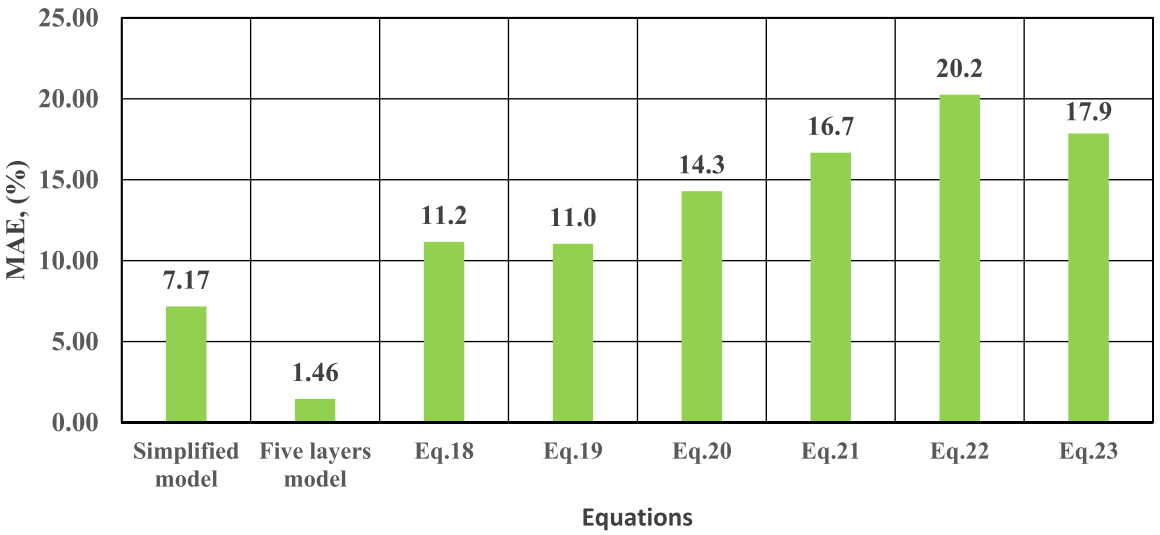

Fig. 14. Mean absolute error values for developed equations and equations 18–23 in predicting dusty PV temperature.

the work reported in this paper.

References

[1] M. Al-Housani, Y. Bicer, M. Koç, Experimental investigations on PV cleaning of large-scale solar power plants in desert climates: comparison of cleaning techniques for drone retrofitting, Energ. Conver. Manage. 185 (2019) 800–815.

[2] H.M. Almukhtar, et al., Feasibility study of achieving reliable electricity supply using hybrid power system for rural primary schools in iraq: a case study with umm qasr primary school, Int. J. Electr. Comput. Eng. 9 (4) (2019) 2822–2830.

[3] H.M. Khalid, et al., Dust accumulation and aggregation on PV panels: an integrated survey on impacts, mathematical models, cleaning mechanisms, and possible sustainable solution, Sol. Energy 251 (2023) 261–285.

[4] F. Ekinci, et al., Experimental investigation on solar PV panel dust cleaning with solution method, Sol. Energy 237 (2022) 1–10.

[5] S.O. Fadlallah, D.E.B. Serradj, Determination of the optimal solar photovoltaic (PV) system for Sudan, Sol. Energy 208 (2020) 800–813.

[6] Hari Om Prasad, S.S. Kalikinkar Mahanta, Sreekanth Bojjagani, Evaluation of particle pollution influence on loss of solar power generation between commercial and background areas in Lucknow, India, Environ. Dev. Sustain. (2023).

[7] M. Abderrezek, M. Fathi, Effect of dust deposition on the performance of thin film solar cell, Elektron Elektrotech 24 (1) (2018) 41–45.

[8] Abhishek Rao, Rohit Pillai, Monto Mani, Praveen Ramamurthy, Influence of dust deposition on photovoltaic panel performance, in: Energy Procedia, Elsevier Ltd, 2014, pp. 690–700.

[9] H. Almukhtar, et al., Comprehensive review of dust properties and their influence on photovoltaic systems: electrical, optical, thermal models and experimentation techniques, Energies 16 (8) (2023).

[10] V. Gupta, M.D. Sharma, R.K. Pachauri, K.N. Dinesh Babu, Comprehensive review on effect of dust on solar photovoltaic system and mitigation techniques, Sol. Energy 191 (2019) 596–622.

[11] M. Dida, S. Boughali, D. Bechki, H. Bouguettaia, Output power loss of crystalline silicon photovoltaic modules due to dust accumulation in saharan environment, Renew. Sustain. Energy Rev. 124 (2020).

[12] A.B. Ahmadullah, et al., A techno-economic review of dust accumulation and cleaning techniques for solar energy harvesting devices, Arab. J. Sci. Eng. (2023).

[13] A.A. Hachicha, E.M. Abo-Zahhad, Dust effect on solar energy systems and mitigation methods, Int. J. Energy Prod. Manag. 8 (2) (2023) 97–105.

[14] M. Almaktar, H.A. Rahman, M.Y. Hassan, S. Rahman, Climate-based empirical model for PV module temperature estimation in tropical environment, Appl. Solar Energy (english translation of Geliotekhnika) 49 (4) (2013) 192–201.

[15] M. Akhsassi, et al., experimental investigation and modeling of the thermal behavior of a solar PV module, Sol. Energy Mater. Sol. Cells 180 (2018) 271–279.

[16] Amir Al-Ahmed, Inamuddin, Fahad A. Al-Sulaiman, Firoz Khan, Green Energy and Technology The Effects of Dust and Heat on Photovoltaic Modules: Impacts and Solutions, 2002, http://www.springer.com/series/8059.

[17] T. Salamah, et al., Effect of dust and methods of cleaning on the performance of solar PV module for different climate regions: comprehensive review, Sci. Total Environ. 827 (2022).

[18] T. Schott, Operation temperatures of PV modules: a theoretical and experimental approach, EC Photovoltaic Solar Energy Conf. 6 (1985) 392–396.

[19] D.L. King, Photovoltaic module and array performance characterization methods for all system operating conditions, in: AIP Conference Proceedings, American Institute of Physics, 1997, pp. 347–368.

[20] Z. Ren, et al., PVLab: an innovative and flexible simulation tool to better size photovoltaic units, Renew. Energy Power Quality J. 1 (12) (2014) 87–91.

[21] V. Tomar, G.N. Tiwari, T.S. Bhatti, B. Norton, Thermal modeling and experimental evaluation of five different photovoltaic modules integrated on prototype test cells with and without water flow, Energ. Conver. Manage. 165 (2018) 219–235.

[22] Y. Tripanagnostopoulos, M. Souliotis, R. Battisti, A. Corrado, Energy, cost and LCA results of PV and hybrid PV/T solar systems, Prog. Photovolt. Res. Appl. 13 (3) (2005) 235–250.

[23] King, David L, Jay A Kratochvil, William Earl Boyson. Photovoltaic Array Performance Model. Citeseer, 2004, 8.

[24] Jean Michel Servant, Calculation of the Cell Temperature for Photovoltaic Modules From Climatic Data, Pergamon Press, 1986, pp. 1640–1643.

[25] A.M. Muzathik, Photovoltaic modules operating temperature estimation using a simple correlation, Int. J. Energy Eng. 4 (August 2014) (2014) 151–158.

[26] V.v. Risser, M.K. Fuentes. Linear regression analysis of flat-plate photovoltaic system performance data, in: 5th Photovoltaic Solar Energy Conference, 1984, pp. 623–27.

[27] Tamizhmani, Govindasamy et al. Photovoltaic Module Thermal/Wind Performance: Long -Term Monitoring and Model Development for Energy Rating, 2003.

[28] R. Chenni, M. Makhlouf, T. Kerbache, A. Bouzid, A detailed modeling method for photovoltaic cells, Energy 32 (9) (2007) 1724–1730.

[29] C. Coskun, N. Koçyiğit, Z. Oktay, YapaSïnïr Ağlarïle Pv Modül Yüzey SicakliğiniTahmïnï, Mugla J. Sci. Technol. 2 (2) (2016) 15.

[30] D. Faiman, Assessing the outdoor operating temperature of photovoltaic modules, Prog. Photovolt. Res. Appl. 16 (4) (2008) 307–315.

[31] A.G. Gaglia, et al., Energy efficiency of PV panels under real outdoor conditions–an experimental assessment in Athens, Greece, Renew. Energy 101 (2017) 236–243.

[32] E. Skoplaki, A.G. Boudouvis, J.A. Palyvos, A Simple correlation for the operating temperature of photovoltaic modules of arbitrary mounting, Sol. Energy Mater. Sol. Cells 92 (11) (2008) 1393–1402.

[33] M.A. Green, et al., Solar cell efficiency tables (Version 40), IEEE Trans. Fuzzy Syst. 20 (6) (2014) 1114–1129.

[34] Ali Sohani, Hoseyn Sayyaadi, Employing genetic programming to find the best correlation to predict temperature of solar photovoltaic panels, Energ. Conver. Manage. 224 (2020).

[35] S. Jacques, et al., Impact of the cell temperature on the energy efficiency of a single glass PV module: thermal modeling in steady-state and validation by experimental data, Renew. Energy Power Quality Journal 1 (11) (2013) 291–294.

[36] M. Mattei, et al., Calculation of the polycrystalline PV module temperature using a simple method of energy balance, Renew. Energy 31 (4) (2006) 553–567.

[37] A. Jha, P.P. Tripathy, Heat transfer modeling and performance evaluation of photovoltaic system in different seasonal and climatic conditions, Renew. Energy 135 (2019) 856–865.

[38] P. Bevilacqua, S. Perrella, R. Bruno, N. Arcuri, An accurate thermal model for the PV electric generation prediction: long-term validation in different climatic conditions, Renew. Energy 163 (2021) 1092–1112.

[39] A.N. Al-Shamani, et al., Mathematical and experimental evaluation of thermal and electrical efficiency of PV/T collector using different water based nano-fluids, Energy 145 (2018) 770–792.

[40] S. Algarni, D. Nutter, Influence of dust accumulation on building roof thermal performance and radiant heat gain in hot-dry climates, Energ. Buildings 104 (July) (2015) 181–190.

[41] K. Yaman, G. Arslan, A detailed mathematical model and experimental validation for coupled thermal and electrical performance of a photovoltaic (PV) module, Appl. Therm. Eng. 195 (2021).

[42] Secchi, Riccardo et al., Effect of a Back Surface Roughness on Annual Performance of an Air-Cooled PV Module Modelling of Coking Process View Project Modelling of Casting Processes View Project Effect of a Back Surface Roughness on Annual

Performance of an Air-Cooled PV Module, 2016, https://www.researchgate.net/publication/268370696.
[43] A.H. Alami, et al., Management of potential challenges of PV technology proliferation, Sustainable Energy Technol. Assess. 51 (2022).
[44] D. Nissenbaum, R. Sarafian, Y. Rudich, S. Raveh-Rubin, Six types of dust events in eastern mediterranean identified using unsupervised machine-learning classification, Atmos. Environ. 309 (2023), 119902.